

Fundamental analysis of the cutting edge micro-geometry in orthogonal machining of unidirectional Carbon Fibre Reinforced Plastics (CFRP)

Conference Paper**Author(s):**

[Seeholzer, Lukas](#) ; Voss, Robert; Grossenbacher, Frank; Kuster, Friedrich; Wegener, Konrad

Publication date:

2018

Permanent link:

<https://doi.org/10.3929/ethz-b-000303269>

Rights / license:

[Creative Commons Attribution-NonCommercial-NoDerivatives 4.0 International](#)

Originally published in:

Procedia CIRP 77, <https://doi.org/10.1016/j.procir.2018.09.040>

8th CIRP Conference on High Performance Cutting (HPC 2018)

Fundamental analysis of the cutting edge micro-geometry in orthogonal machining of unidirectional Carbon Fibre Reinforced Plastics (CFRP)

Lukas Seeholzer^{a,*}, Robert Voss^a, Frank Grossenbacher^a, Friedrich Kuster^a, Konrad Wegener^a

^a Institute of Machine Tools and Manufacturing (IWF), ETH Zurich, Leonhardstrasse 21, 8092 Zurich, Switzerland

* Corresponding author. Tel.: +41 44 6325309; fax: +41 446320731. E-mail address: seeholzer@iwf.mavt.ethz.ch

Abstract

Machining of carbon fibre reinforced plastics (CFRP) is closely related to strong abrasive tool wear and represents a significant process challenge due to its anisotropic material structure and brittle fracture behavior. Furthermore, machining of unidirectional CFRP material shows a significant increase in process forces due to tool wear effects, resulting in a changing micro-geometry of the cutting edge. This research work aims to give a detailed analysis of the tool wear behavior with respect to the five micro-geometry parameters based on an approach of “straight line–ellipse–straight line”, capable also to describe the developing asymmetric cutting edge. Therefore, fundamental orthogonal machining experiments with varying fibre orientations and tool geometries are conducted. It can be shown that the micro-geometry changes with increasing cutting length, whereby an increase of the resulting friction length and spring back height can be detected, having a significant influence on the process forces.

© 2018 The Authors. Published by Elsevier Ltd.

This is an open access article under the CC BY-NC-ND license (<https://creativecommons.org/licenses/by-nc-nd/4.0/>)

Selection and peer-review under responsibility of the International Scientific Committee of the 8th CIRP Conference on High Performance Cutting (HPC 2018).

Keywords: Fiber reinforced plastic; Cutting edge; Wear; Machine Tool; Turning

1. Introduction

Carbon fibre reinforced plastics (CFRP) with their high specific strength and stiffness properties represent a high potential for lightweight constructions, such as those found in aerospace applications. Simultaneously, machining of CFRP is still a great challenge due to the distinct tool wear and the inhomogeneous microstructure, resulting in an anisotropic material behavior. Various researchers [2, 3, 5, 6] showed a strong correlation between the wear-induced cutting edge rounding and the occurring machining defects and process forces. This paper deals with a detailed analysis of the tool wear due to the abrasive carbon fibres, resulting in an increasing cutting edge rounding.

With respect to the occurring tool wear KOPLEV et al. [7] conducted orthogonal machining experiments with unidirectional CFRP and stated a significant increase of the process forces as a result of the wear-induced cutting edge

rounding. Subsequently, HENERICHS [3] conducted various orthogonal machining experiments with unidirectional CFRP and detected an asymmetric cutting edge rounding, whereby its intensity strongly depends on the initial tool geometry and the machined fibre orientation. WANG et al. [9] described mechanical wear as the dominant wear mechanism in machining CFRP, while further wear mechanisms as diffusion and dissolution can be excluded due to the low process temperatures. Furthermore, WANG et al. [9] explained the mechanical abrasion by the absence of a stagnation zone in front of the cutting edge. This stagnation zone, which is well known in metal machining, represents an accumulation of workpiece material, acting like a protection for the cutting edge. According to WANG et al. [9] the relative motion between the cutting edge and the workpiece is significantly reduced by the stagnation zone, whereby in accordance to ARCHARD [1] the intensity of mechanical abrasion decreases. In accordance to VOSS [8] tool wear primarily affects a small

region next to the cutting edge. This so-called micro-geometry describes the transition between the flank and the rake face. During CFRP machining, a tool-sided material removal due to mechanical abrasion occurs, resulting in a distinct change of the micro-geometry. In order to quantify the corresponding cutting edge rounding, VOSS [8] proposed a simplified description of the contact region by five micro-geometry parameters (l_α , l_γ , γ^* , α^* , b_c), which will be explained in detail below. Therefore, it will be shown, that the operative part of the cutting edge can be sufficiently described by the simplification «straight line – ellipse – straight line», see Figure 1. For this purpose the cutting edge is subdivided into three separate regions according to ZHANG et al. [10].

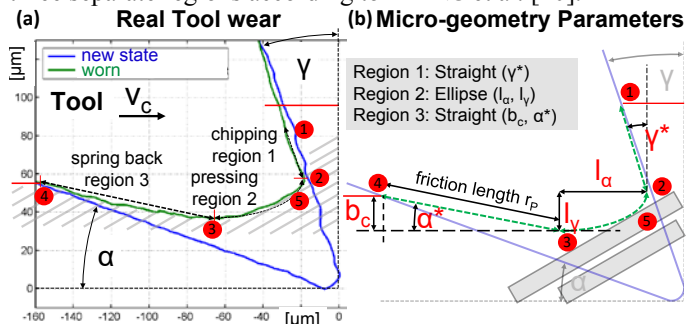


Figure 1: (a) Exemplary new and worn cutting edge profile and (b) evaluation of worn micro-geometry with five micro-geometry parameters [8]

The *chipping region 1* along the rake face is bounded by the nominal material level ahead of the cutting edge 1 and the most forward point in cutting velocity direction 2. With increasing tool wear this region is assumed to stay straight but with a changing rake angle γ^* . The *pressing region 2* represents the contact length along the cutting edge rounding between the most forward point in cutting velocity direction 2 and feed direction 3 respectively. The tool shape in region 2 can sufficiently be described by an ellipse with the semi-major axes l_α and l_γ . The *spring back region 3* represents the contact length of the flank face between the most forward point in feed direction 3 and the profile separation point 4. The latter defines the transition between the new and the worn profile, whereby the distance in feed direction between 3 and 4 corresponds to the spring back height b_c , which results from the elastic spring-back of the material. In combination with α^* , the parameter b_c defines the friction length r_p and thus the straight in region 3.

2. Experimental Setup and material

To analyse the increasing tool wear in orthogonal machining CFRP, fundamental machining experiments with four different tool geometries and two fibre orientations for an overall cutting length of $l_g=35$ m are conducted on a CNC lathe *Okuma LB15-II*. The notation of the fibre orientation angle correspond to that of HENERICHS et al. [4]. For the experiments CFRP in form of three 120° angular ring segments (55 mm width, 5 mm wall thickness, 200 mm radius) are combined and fixed by modified clamping jaws on a hydraulic chuck, see Figure 2. To avoid a deflection of the CFRP ring element due to the high clamping forces, an inner aluminum ring is used, as shown by HENERICHS et al. [4].

With this test-rig a non-interrupted orthogonal machining process is achieved, while the fibre orientation, the cutting speed $v_c=90$ m/min, the feed rate $f=0.03$ mm/rev and the width of cut $a_c=5$ mm are constant. To avoid issues due to powder like CFRP chips a suction unit of the type *AL-KO PowerUnit120/400* is used. In order to enable online measuring of the process forces a 3D-dynamometer of the type *Kistler 9121* is applied. The unidirectional CFRP material used for the turning experiments has the specification *M21/34%/UD194/IMA-12k* and is widely used in the aerospace industry [4]. It consists of 41% high performance matrix material *HexPly® M21* and 59% carbon fibres *IMA-12k*. In accordance to HENERICHS et al. [4], machining this material represents a big challenge due to both the high fibre content as well as the high toughness of the fibre-matrix-system which cause extensive tool wear.

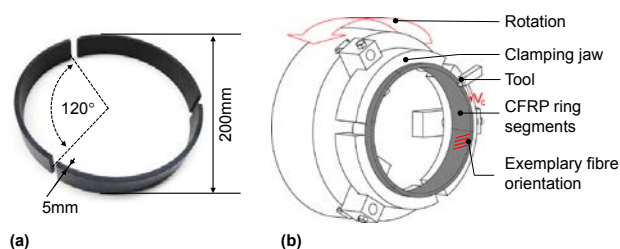


Figure 2: (a) segmented ring specimen and (b) schematic illustration of the test-rig setup for orthogonal cutting experiments

A detailed summary of the physical and mechanical properties of the CFRP material is presented by HENERICHS et al. [4]. For the turning experiments, uncoated carbide cutting inserts of the grade H13A are used. To investigate different combination of rake and clearance angles, the initial cutting insert geometry CCMW09T304 (ISO standards) is adjusted by additional grinding operations.

3. Measurement of tool wear

To analyse the cutting edge rounding as a result of the increasing tool wear, the orthogonal machining process is interrupted in regular intervals and the actual wear state of the cutting edge is analysed by means of optical microscopy using an *Alicona Infinite Focus* microscope. In order to reduce the influence of outlier values, each turning experiment is conducted twice. In addition to the initial micro-geometry ($l_g=0$ m) the following wear states are analysed: $l_g=5$ m, $l_g=10$ m, $l_g=15$ m, $l_g=20$ m and $l_g=35$ m. In each wear state the five micro-geometry parameters (l_α , l_γ , γ^* , α^* , b_c) are evaluated by means of a modified *Cutting Edge Analyser* (CEA) [4]. In order to determine the spring back height b_c , the transition point 4 between the new and the worn cutting tool is crucial. To enable a repeatable evaluation of this transition point, the flank face of the cutting insert is marked by a short pulsed *Yb*-laser of the type *IPG YLP-HP*. For this, the following laser parameter are used: Power of 14 W, wavelength 1064 nm, pulse frequency 100 kHz, pulse duration 125 ns and scanner feed 1200 mm/s. As shown in Figure 3 (a), the marking lines on the flank face are arranged in form of a grid, where the distance between the corresponding lines parallel and perpendicular to the cutting edge are 100 μ m and 500 μ m

respectively. The resulting depth of the laser marks is so small that they vanish if they get in contact with the spring-back CFRP-material. Figure 3 (b) shows the shift of the transition line due to increasing tool wear resulting in an increasing friction length in region 3.

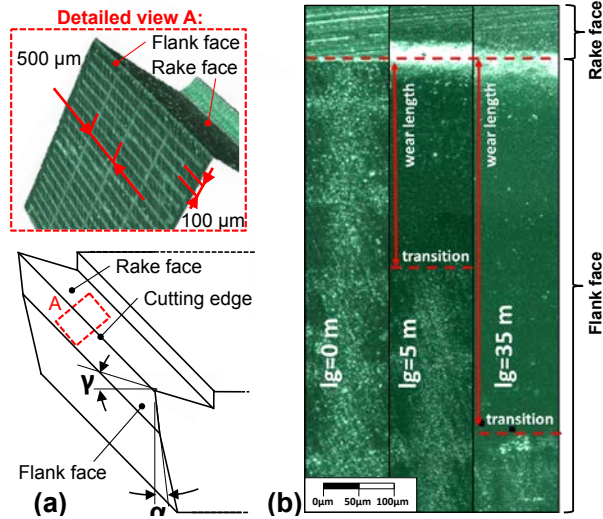


Figure 3: (a) Laser marking grid on the flank face and (b) shift of the transition line due to mechanical wear

4. Experimental Results

In the following the trends of the five micro-geometry parameters (l_α , l_γ , γ^* , α^* , b_c) are discussed in detail with respect to the three regions of the cutting edge. The presented results include the fibre orientations $\theta=30^\circ$ and $\theta=60^\circ$ and the following four tool geometries: J ($\gamma=20^\circ, \alpha=7^\circ$), L ($\gamma=20^\circ, \alpha=14^\circ$), M ($\gamma=20^\circ, \alpha=21^\circ$) and H ($\gamma=10^\circ, \alpha=14^\circ$). While the tools J, L and M differ only in terms of the initial clearance angle, the tool H has a smaller initial rake angle, but otherwise corresponds to the tool L. Based on the geometric description of the micro-geometry which is explained in section 1, the wear-induced change of the micro-geometry in region 1 is described by the parameter γ^* . This parameter represents the rake angle, which is changed by a wear-induced material removal on the rake face. The graphs in Figure 4 show the trend of γ^* for the four tool geometries during machining $\theta=30^\circ$ and $\theta=60^\circ$ material for an overall cutting length of $l_g=35$ m.

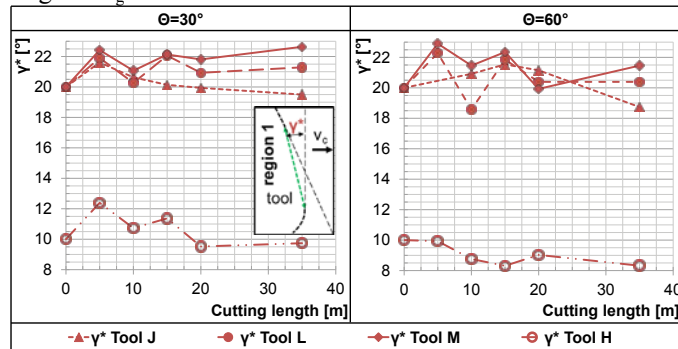


Figure 4: Trend of γ^* with increasing cutting length for different tool geometries in $\theta=30^\circ$ and $\theta=60^\circ$ material; $v_c=90$ m/min and $f=0.03$ mm/rot

Figure 4 shows that for both $\theta=30^\circ$ and $\theta=60^\circ$, the dimension of the resulting rake angle γ^* is primarily affected by the initial rake angle γ . Furthermore, Figure 4 implies a wear-induced change of the parameter γ^* with increasing cutting length. In terms of the tools with varying initial clearance angles (J, L and M) the wear-induced changes are small. In combination with an overall measuring accuracy of $\pm 3^\circ$ no distinct conclusion about the influence of both the clearance and rake angle is possible.

The micro-geometrical shape in region 2 is modelled as an ellipse, described by the two semi-major axes l_α and l_γ . Figure 5 shows the trends of these two parameters for the respective tool geometries and fibre orientations over the cutting length of $l_g=35$ m. Fundamentally, it can be stated that all tool geometries for both fibre orientations show a similar trend of the parameters l_α and l_γ . Starting from the initial circular shape ($l_\alpha=l_\gamma$), the increase of l_α is significantly higher than of l_γ , resulting in an increasing asymmetric shape of the cutting edge in region 2. In the scope of the tested tools and fibre orientations, no clear influence of the initial tool geometry to the resulting trends of l_α and l_γ is detected. Furthermore, the appropriate trends of l_α and l_γ are characteristic and could be well approximated by a root function which includes a significant influence of the actual fibre orientation.

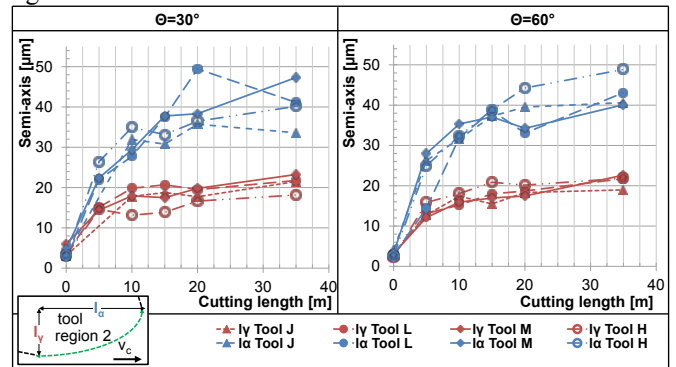


Figure 5: Trend of l_γ and l_α with increasing cutting length for different tool geometries in $\theta=30^\circ$ and $\theta=60^\circ$ material; $v_c=90$ m/min and $f=0.03$ mm/rot

According to the previous results, Figure 6 shows the trends of the parameters α^* and b_c , which describe the wear-induced change of the micro-geometry in region 3. Although the parameter α^* primarily depends on the initial clearance angle, significantly different trends are determined for the tools J, L and M. In this context the extrapolated trends of α^* , which are shown in Figure 6 by dotted black lines, imply that all clearance angles converge to a single constant clearance angle in the worn state of the cutting edge. The fact, that this limit value is different for the fibre orientations $\theta=30^\circ$ and $\theta=60^\circ$ indicate a dependency of the convergence behavior on the fibre orientation angle. This fact could be explained by different chip formation effects due to a different relative positioning of the fibre with respect to the tool. According to Figure 6, the higher the initial clearance angle, the more distinct is the wear-induced decrease of the parameter α^* per cutting length. Based on the nearly similar trends of the parameter α^* for the tools L and H, the effect of the initial rake angle is not significant and thus negligible. The trends of the parameter b_c show a crucial influence of the initial

clearance angle and the fibre orientation, while the influence of the initial rake angle is approximately neglectable. The tool J with the smallest initial clearance angle shows the largest increase of b_c and the tool M with the lowest initial clearance angle the smallest increase. Furthermore, the increase of the fibre orientation angle from $\theta=30^\circ$ to $\theta=60^\circ$ results especially for the tool J with the lowest initial clearance angle in an overall lower spring back height b_c .

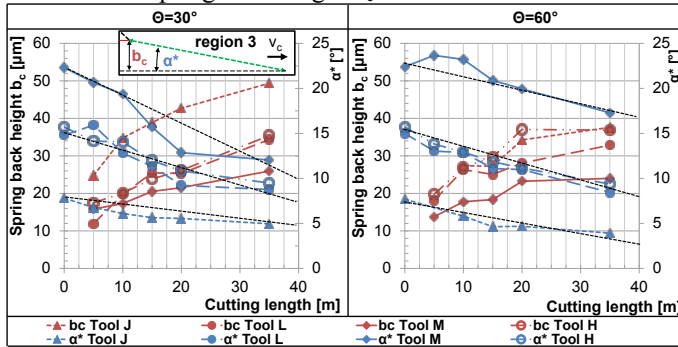


Figure 6: Trend of α^* and b_c with increasing cutting length in $\theta=30^\circ$ and $\theta=60^\circ$ material; $v_c=90$ m/min and $f=0.03$ mm/rot

The results in Figures 4, 5 and 6 show a distinct change of the micro-geometrical shape with increasing cutting length up to $l_g=35$ m. Furthermore, the dependencies of the wear-induced change on the initial tool geometry and the fibre orientation are different with respect to the three regions of the cutting edge. While the tool wear in regions 1 and 2 is nearly similar, region 3 significantly depends on both the initial clearance angle and the fibre orientation. Since the corresponding thrust forces also clearly diverge, a strong correlation with the wear in region 3 is assumed. In this context, Figure 7 (a) shows the trends of the thrust force exemplary for $\theta=30^\circ$ and the tools J, L and M. Basically, the smaller the initial clearance angle, the higher the wear-induced increase in the corresponding thrust force. This fact can be explained by a detailed analysis of the thrust force relevant areas of the cutting edge and its influence factors.

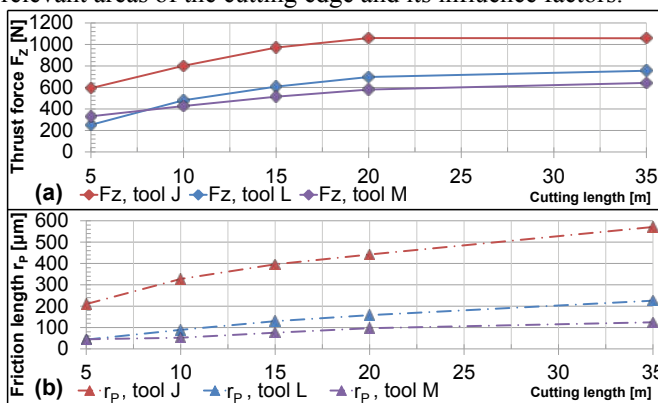


Figure 7: Trend of r_p , l_a and the thrust forces with increasing cutting length in $\theta=30^\circ$ material; $v_c=90$ m/min and $f=0.03$ mm/rot

Since the thrust force primarily depends on the contact area between the tool and the just machined workpiece surface, the regions 2 and 3 have to be considered. As mentioned above, the influence of the initial clearance angle on the micro-geometrical shape in region 2 is low and thus also its share to

the resulting thrust forces. In contrast, the share of region 3, defined as the subarea A_C has a huge influence and strongly depends on the initial clearance angle. This subarea A_C can be determined by multiplying the friction length r_p and the cutting width, which corresponds to the constant wall thickness b . Figure 7 (b) shows the trend of the friction length with increasing cutting length. Due to the fact that the thrust forces show nearly comparable trends, it can be concluded that region 3 is primarily responsible for the increasing thrust forces during machining CFRP. The evaluation of $\theta=60^\circ$ is not shown here, but yields an equivalent characteristic.

5. Conclusion

In the scope of this paper, a detailed analysis of the wear-induced cutting edge rounding in case of orthogonal machining unidirectional CFRP is presented. The trends of the five micro-geometry parameters (l_a , l_y , γ^* , α^* , b_c) are shown for different fibre orientations and tool geometries. Additionally, a suitable measurement method is presented to predict the spring back height of the CFRP material and thus the resulting friction length. Furthermore, the friction length in region 3, which is significantly influenced by the fibre orientation and the initial clearance angle is stated as the main influence factor for the distinct increases of the thrust forces.

Acknowledgements

The authors thank the Commission for Technology and Innovation (CTI Project 18309.2 PFIW-IW), the companies Dixi Polytool SA, Heule Werkzeuge AG and Oerlikon Surface Solutions AG for the support.

References

- [1] Archard J. F., Contact and Rubbing of Flat Surfaces. Journal of Applied Physics, 1953. 24(981).
- [2] Chen W.-C., Some experimental investigations in the drilling of carbon fiber-reinforced plastic (CFRP) composite laminates. International Journal of Machine Tools and Manufacture, 1997. 37(8): p. 1097-1108.
- [3] Henerichs M., Bohrbearbeitung von CFK unter besonderer Berücksichtigung der Schneidkantenmikrogeometrie. 2015, Eidgenössische Technische Hochschule Zürich (ETH): Zürich.
- [4] Henerichs M., Voss R., Kuster F., Wegener K., Machining of carbon fiber reinforced plastics: Influence of tool geometry and fiber orientation on the machining forces. CIRP Journal of Manufacturing Science and Technology, 2015. 9: p. 136-145.
- [5] Hocheng H., Puw H., On drilling characteristics of fiber-reinforced thermoset and thermoplastics. International Journal of Machine Tools and Manufacture, 1992. 32(4): p. 583-592.
- [6] Hocheng H., Tsao C., Comprehensive analysis of delamination in drilling of composite materials with various drill bits. Journal of Materials Processing Technology, 2003. 140(1): p. 335-339.
- [7] Koplev A., Lystrup A., Vorm T., The cutting process, chips, and cutting forces in machining CFRP composites, 1983. 14(4): p. 371-376.
- [8] Voss R., Fundamentals of Carbon Fibre Reinforced Polymer (CFRP) Machining. 2017, Eidgenössische Technische Hochschule Zürich (ETH): Zürich.
- [9] Wang X., Kwon P. Y., Sturtevant C., Lantrip J., Tool wear of coated drills in drilling CFRP. Journal of Manufacturing Processes, 2013. 15(1): p. 127-135.
- [10] Zhang L. C., Zhang H. J., Wang X. M., A force prediction model for cutting unidirectional fibre-reinforced plastics. Machining Science and Technology, 2001. 5(3): p. 293-305.